Substrate adaptability of β-lactamase

Sun, J.

Chapter 4

Directed evolution enhances ceftazidime activity of BlaC by stabilization of an open state

Introduction

The results in Chapters 2 and 3 led to the conclusion that ceftazidime hydrolysis can readily be enhanced by a single mutation, P167S (chapter 2), or increase in the pH to alkaline conditions (chapter 3). In both cases, an open state of the enzyme becomes more populated and is more active against this substrate. However, the catalytic efficiency remains low compared to that of WT BlaC for other substrates, such as ampicillin and nitrocefin. Still, it serves as an example of the first step of evolution toward a new functionality of an enzyme. If selection pressures change, organisms adapt by using existing proteins to acquire new functions by mutations. Even if the activity against a new antibiotic is low initially, it can lead to an evolutionary advantage allowing for further improvement to occur. In this chapter, the evolutionary adaptability of BlaC is tested by applying directed evolution to determine whether ceftazidime activity can be enhanced further. By comparing the activity of the new variants for nitrocefin hydrolysis, a potential activity trade-off can also be detected.

Enzymes must find a balance between activity and stability. Acquisition of new functions requires adaptation of the structure, which is often accompanied by reduced stability. Thus, it can be expected that evolution at low temperatures is more permissive because the stability of the folded state goes down with increasing temperature. In other words, temperature can act as an accompanying selection pressure in evolution. However, unfolding is highly cooperative and, therefore, happens over a small temperature trajectory. In this chapter, BlaC was evolved at two temperatures to determine whether it would lead to different outcomes and yield variants optimized for the temperature at which evolution took place.

It is found that four rounds of directed evolution lead to a dramatic increase in the catalytic efficiency for ceftazidime, at the cost of nitrocefin activity. Interestingly, stability, as measured by the melting temperature, goes down in the first step(s) of evolution and then increases, even when evolution takes place at low temperatures. The variants evolved at low temperatures are not optimized for that temperature, but rather are more active at higher temperatures. However, they are more active at low

temperature than variants evolved at high temperature. Structural analysis shows that the directed evolution selects mutations that stabilize selectively the most active state of the enzyme, reducing the entropy introduced by the first step of the evolution.

Results

BlaC can readily be evolved to high ceftazidime activity.

In a screen at 30 °C for *blaC* mutants with improved ceftazidime resistance in an *Escherichia coli* expression system,[211] the BlaC variant P167S/D240G (PD) was identified, exhibiting a 16-fold better resistance than the wild-type on ceftazidime at the same temperature *in vivo*. It displayed comparable resistance to ceftazidime at 23 °C and 37 °C (Table S4.1). *In vitro*, the P167S/D240G (PD) showed 40-fold higher k_{cat}/K_M than the wild type and a trade-off in nitrocefin activity is observed, going down ~17-fold (Table 4.2). To test how resistance would further evolve and with which trade-offs, error-prone PCR of *blaC* gene of the variant P167S/D240G was performed to create a first-generation library. Then three generations (G1-G3) of directed evolution were performed at 23 °C and 37 °C, using increasing ceftazidime concentrations (Figure 4.1). A screen sampled 10^6 to 10^8 clones per generation. The G1 screen at 23 °C yielded mutant P167S/D240G/T208I/T216A (PDTT). In G2 mutation I105F was acquired (PDTTI) and in G3 D176G (PDTTID). G1 at 37 °C yielded two variants, and each was evolved further, yielding P167S/D240G//D172A/S104G/H184R (PDDSH) and P167S/D240G/I105F/H184R (PDIH) in G3, respectively. The PDIH variant was sufficiently resistant to skip the conditions of G2.

To compare the sensitivity of the evolved variants for ceftazidime accurately, drops of *E. coli* cell cultures of OD_{600} 0.3 to 0.0003 were applied on agar plates with ceftazidime (Figure 4.2a, Figure S4.1 & S4.2). The minimum inhibitory concentration (MIC) is defined as the concentration at which no growth was visible in this assay. The results indicate that the mutants evolved at 37 °C display a more than 15-fold increased resistance than PD and over 120-fold more than the WT after three rounds of directed evolution (Table S4.1), which is quite remarkable, given that ceftazidime is considered a very poor substrate for BlaC and many other class A β-

lactamases. The mutants that evolved at 37 °C exhibited lower resistance to ceftazidime at 23 °C. Interestingly, also the mutants evolved at 23 °C showed better resistance to ceftazidime at 37 °C than at 23 °C (Figure 4.2a). However, mutants originating from low-temperature evolution show better resistance at low temperatures than those derived from high-temperature evolution, suggesting that the variants evolved at low temperatures are more optimized for this condition.

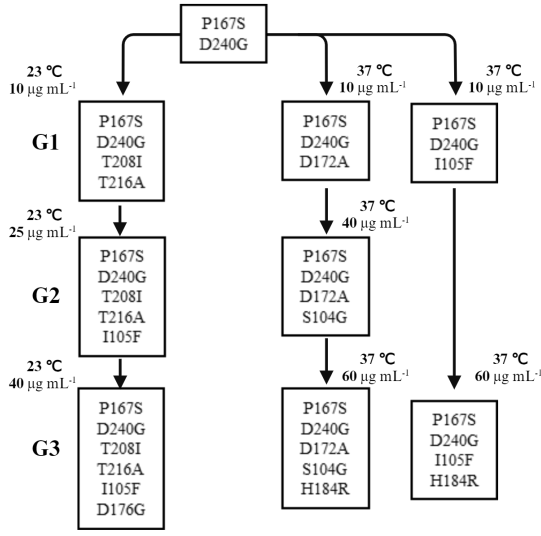

Figure 4.1 Schematic representation of the directed evolution and obtained variants. Amino acid mutations obtained in successive generations are shown and the ceftazidime concentration used for selection is indicated.

Table 4.1 Melting temperatures for BlaC variants. SD represents the standard deviation over three measurements. G, Generation; Temp, temperature at which variant was evolved, T_m, melting temperature.

BlaC variant	G	Temp (℃)	T_m (SD) (℃)	ΔT_m (SD) (℃)
WT			62.0 (0.1)	-
P167S/D240G (template)	0	30	52.8 (0.1)	0
P167S/D240G/T216A/T208A (PDTT)	1	23	50.7 (0.2)	-2.1 (0.2)
P167S/D240G/T216A/T208A/I105F (PDTTI)	2	23	52.6 (0.2)	-0.2 (0.2)
P167S/D240G/T216A/T208A/I105F/D176G (PDTTID)	3	23	53.8 (0.3)	1.0 (0.3)
P167S/D240G/D176G (PDD)	1	37	54.0 (0.1)	1.2 (0.1)
P167S/D240G/D176G/S104G (PDDS)	2	37	55.3 (0.1)	2.5 (0.1)
P167S/D240G/D176G/S104G/H184R (PDDSH)	3	37	57.5 (0.1)	4.7 (0.1)
P167S/D240G/I105F (PID)	1	37	55.0 (0.1)	2.2 (0.1)
P167S/D240G/I105F/H184R (PIDH)	3	37	56.8 (0.1)	4 (0.1)

Stability and activity both increase in successive generations.

To characterize the BlaC variants further, the enzymes were overproduced in *E. coli*. The yield of soluble protein varied strongly for the different variants (Figure 4.2b & Figure S4.3). In some steps of the direct evolution the level increases, but the G3 variants do not all have the highest expression level. Thus, it is concluded that the increasing resistance to ceftazidime is not solely a consequence of different levels of soluble enzyme. The thermostability of all purified variants was determined in a Trp fluorescence assay. The parent variant for evolution, PD, showed a melting temperature of 52.8 ℃, a decrease of 9.2 ℃ compared to that of WT BlaC (62 ℃)[188] (Figure S4.4 and Table 4.1). Variant PDTT (G1 at 23 ℃) displayed a 2.1 degree decrease in melting temperature relative to PD, whereas the mutants from G2 (PDTTI) and G3 (PDTTID) at 23 ℃ showed increased melting temperatures (Table 4.1 and Figure 4.2b). Each mutant evolved at 37 ℃ displayed better stability than its parent (Figure 4.2b and Table 4.1).

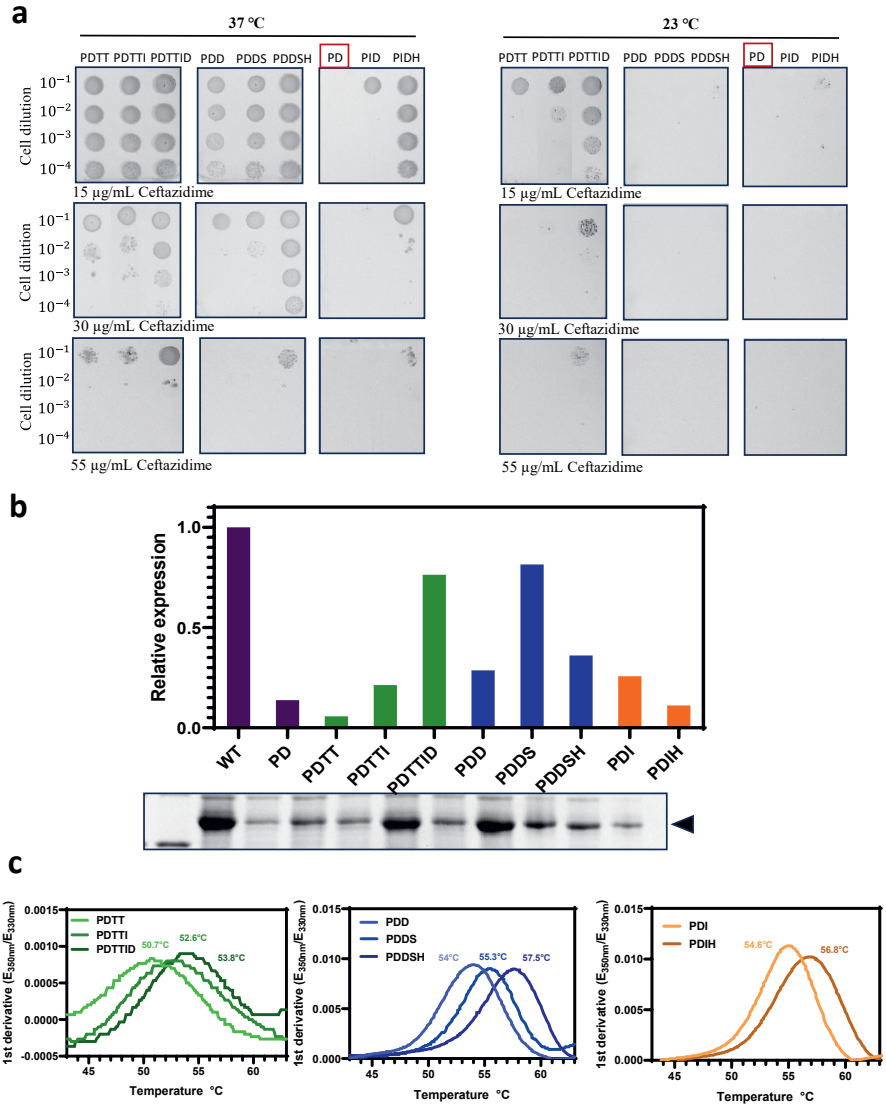

Figure 4.2 Cell growth, protein production and melting temperature. **a)** Drops of increasing dilution of *E. coli* cultures were spotted on LB-agar plates containing ceftazidime and kanamycin (50 µg mL^{-1}) to ensure plasmid stability and 1 mM IPTG to induce gene expression. The plates were incubated at 37 °C and 23 °C until growth was visible. The letters refer to the variants (Table 4.1); **b)** The graph and SDS-PAGE gel represent the levels of soluble BlaC variant levels relative to wild-type BlaC. The full SDS-PAGE gel is shown in Figure S4.4; **c)** The derivative signal from Trp fluorescence as a function of temperature for the BlaC variants,

abbreviated with the amino acid letters of mutated residues. The left panel shows the variants obtained at 23 ℃. The middle and the right panels show those obtained at 37 ℃. The melting temperatures are listed in Table 4.1.

Increased ceftazidime activity reduces nitrocefin activity.

To evaluate the β-lactam resistance profile of the evolved BlaC mutants, kinetic parameters were determined. Increased ceftazidime activity could be accompanied by trade-offs, therefore, both ceftazidime and nitrocefin hydrolysis rates were measured. Initial velocities at different nitrocefin concentrations were determined and fitted to the Michaelis-Menten equation (eq. 4.1). The catalytic efficiencies ($k_{\mathrm{cat}}/K_{\mathrm{M}}$) decrease up to 150-fold for the variants, compared to WT BlaC ($5.6 \pm 0.3 \times 10^5$ $M^{-1}s^{-1}$) (Table 4.2). Similar experiments were performed with ceftazidime. Hydrolysis of 25 μM ceftazidime was measured using 80 nM BlaC for 5 min. Using equation 4.2,[100] the initial velocities were used to estimate the $k_{\mathrm{cat}}/K_{\mathrm{M}}$ value. The third-generation variants demonstrated about 5 to 10-fold increase in catalytic efficiency compared to the parent mutant PD and increased 200-fold over the WT BlaC (Table S4.2 & Figure 4.2b). Thus, improved ceftazidime activity is accompanied by deterioration of the activity on nitrocefin, indicating activity trade-off between these substrates. Interestingly, the catalytic efficiencies for ceftazidime hydrolysis increase monotonously with temperature to 35 °C, equally for the mutants evolved at 23 °C and 37 °C (Figure 4.3b), indicating that the former ones do not suffer from short-term stability problems at this temperature, in line with the in-cell results (Figure 4.2a).

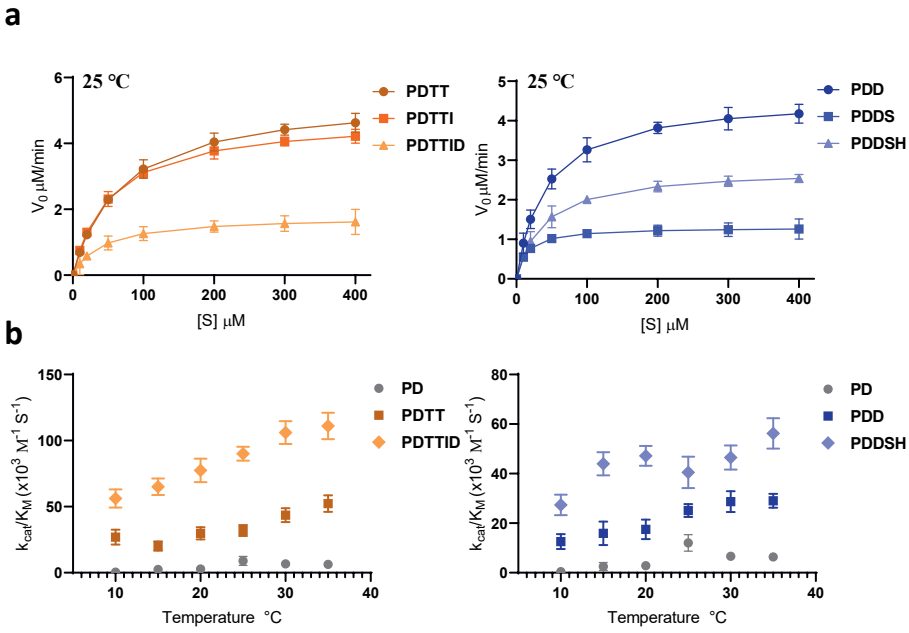

Figure 4.3 Enzyme activities. **a)** Activity curves for nitrocefin hydrolysis; **b)** Temperature dependence of the catalytic efficiencies for ceftazidime hydrolysis. All experiments were performed in 100 mM sodium phosphate buffer, pH 6.4. Error bars represent the standard deviation of three measurements.

Table 4.2 Kinetic parameters for nitrocefin hydrolysis by evolved BlaC variants at 25 °C, 30 °C, and 35 °C. The errors are the standard deviation over three experiments.

BlaC variants	25°C			30°C			35°C		
	k_{cat} (s^{-1})	K_M^{app} (μM)	k_{cat}/K_M^{app} (10^5 $M^{-1}s^{-1}$)	k_{cat} (s^{-1})	K_M^{app} (μM)	k_{cat}/K_M^{app} (10^5 $M^{-1}s^{-1}$)	k_{cat} (s^{-1})	K_M^{app} (μM)	k_{cat}/K_M^{app} (10^5 $M^{-1}s^{-1}$)
Wildtype (WT)	120 ± 8	215 ± 19	5.6 ± 0.6						
P167S/D240G	5.2 ± 0.8	43 ± 6	1.2 ± 0.3						
P167S/D240G/T208I/T216A	0.4 ± 0.1	68 ± 3	0.07 ± 0.02	0.6 ± 0.1	83 ± 21	0.08 ± 0.03	0.9 ± 0.3	131 ± 13	0.07 ± 0.02
P167S/D240G/T208I/T216A/I105F	0.40 ± 0.08	53 ± 1	0.08 ± 0.02	0.5 ± 0.2	56 ± 20	0.09 ± 0.03	0.94 ± 0.05	92 ± 19	0.10 ± 0.02
P167S/D240G/T208I/T216A/I105F/D176G	0.15 ± 0.01	41 ± 3	0.036 ± 0.001	0.17 ± 0.01	47 ± 2	0.036 ± 0.002	0.14 ± 0.02	55 ± 5	0.026 ± 0.005
P167S/D240G/D172A	0.38 ± 0.03	41 ± 11	0.10 ± 0.02	0.44 ± 0.03	41 ± 5	0.11 ± 0.02	0.36 ± 0.08	21± 12	0.20 ± 0.06
P167S/D240G/D172A/S104G	0.11 ± 0.01	14 ± 6	0.08 ± 0.02	0.12 ± 0.01	25 ± 3	0.05 ± 0.01	0.13 ± 0.01	18.3 ± 0.3	0.07 ± 0.01
P167S/D240G/D172A/S104G/H184R	0.23 ± 0.03	39 ± 10	0.06 ± 0.01	0.22 ± 0.04	32 ± 9	0.07 ± 0.01	0.19 ± 0.03	17 ± 3	0.11 ± 0.01
P167S/D240G/I105F/H184R	7.87 ± 0.04	519 ± 5	0.15 ± 0.01	3.10 ± 0.02	117 ± 3	0.26 ± 0.01	3.9 ± 0.2	226 ± 17	0.17 ± 0.01

The active state of the enzyme becomes more populated in successive generations.

To further characterize the structure of the evolved mutant, ^{1}H-^{15}N TROSY-HSQC spectroscopy and HNCA were performed to get the NMR backbone assignments for the evolved BlaC mutants. The NMR data revealed that the template BlaC P167S/D240G exists in two conformations. Peak duplication was also displayed for some of the evolved mutants (Figure 4.4), indicating that the resting enzyme exists in two folded states, undergoing a conformational exchange that is slow on the NMR time scale. An exception is PDD for which only a single state is observed. To aid in distinguishing the two conformations, the spectra of P167S/D240G were overlaid with those of P167S, which also has two states, defined as open and closed states (Chapter 2, Figure 4.4a). In successive steps of the evolution, the cross-peak intensity of one state increases relative to the other. Upon raising the temperature from 10 ℃ to 30 ℃, the population of the main state increases by 3% for PDDS and 10% for PDTTI, which could suggest that the mutant evolved from 37 ℃ is not as sensitive to the temperature change as the mutants from 23 ℃ (Figure 4.4b). Taken together, these data show that most of the mutants exhibit a slow equilibrium between two conformations. In the step from G2 to G3, the population of the less abundant species becomes less populated. The conformation populated most in G3 variants is expected to be the more active state for hydrolysis ceftazidime.

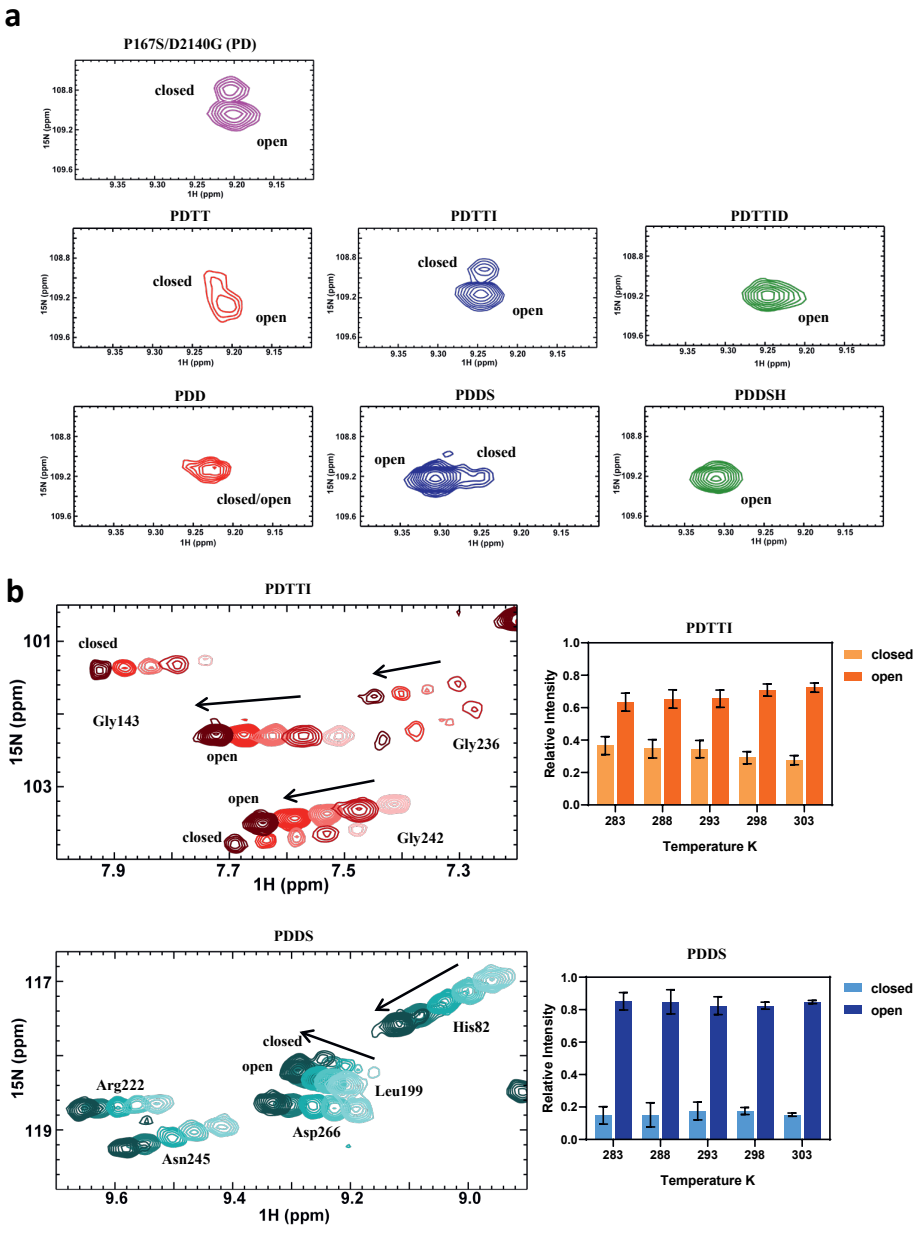

Figure 4.4 Conformation change of the BlaC mutants and temperature effect on G2. **a)** Detail of ^{1}H-^{15}N TROSY-HSQC spectra showing resonances for residue Gly120 of BlaC

P167S/D240G (pink), mutant G1 (red), mutants G2 (navy), and mutants G3 (green) at 25 °C; **b)** Temperature effect on the relative intensity of the two states of G2 mutants. Details of spectra (left) and the relative intensities of the open form and closed form of PDTTI (orange) and PDDS (blue) averaged (and SD) over 10 residues at different temperatures (right). The arrows indicate increasing temperature.

The Ω-loop shows flexibility in the crystal structure of two mutants.

To provide structural information on these conformational evolved BlaC mutants, we performed the x-ray crystallography. The crystal structures of BlaC P167S/D240G and P167S/D240G/D172A/S104G (PDDS) were obtained and solved at 1.3 Å and 1.6 Å resolution, respectively (Table S4.3). The overall structures of the two mutants resemble that of WT BlaC (Figure 4.5a), and their superimposition yields a root mean square deviation (RMSD) of 0.39 Å for C_α atoms. However, significant differences between the two mutants and the WT are observed in the Ω-loop (Figure 4.5a). For PD, the Ω-loop exhibits large positional and conformational changes, resulting in a significant expansion of the active site cavity (Figure 4.5b). In PDDS, the loss of the negatively charged carboxyl group due to the D172A substitution causes disruption of the low-barrier H-bond of D179-D172 (described in Chapter 3) and the Ser167 substitution can also increase the flexibility of the Ω-loop. Residues Leu169 and Asn170 show alternative conformations based on the electron density map (data not shown) and the density from residue 167 - 172 is only partially ordered, suggesting that there is mobility in this region of Ω-loop (Figure 4.5b). The conformational change in the Ω-loop gives ceftazidime better access to the active site. Given that it is the most populated form of PDDS in solution, the crystal structure mostly likely represents the open form.

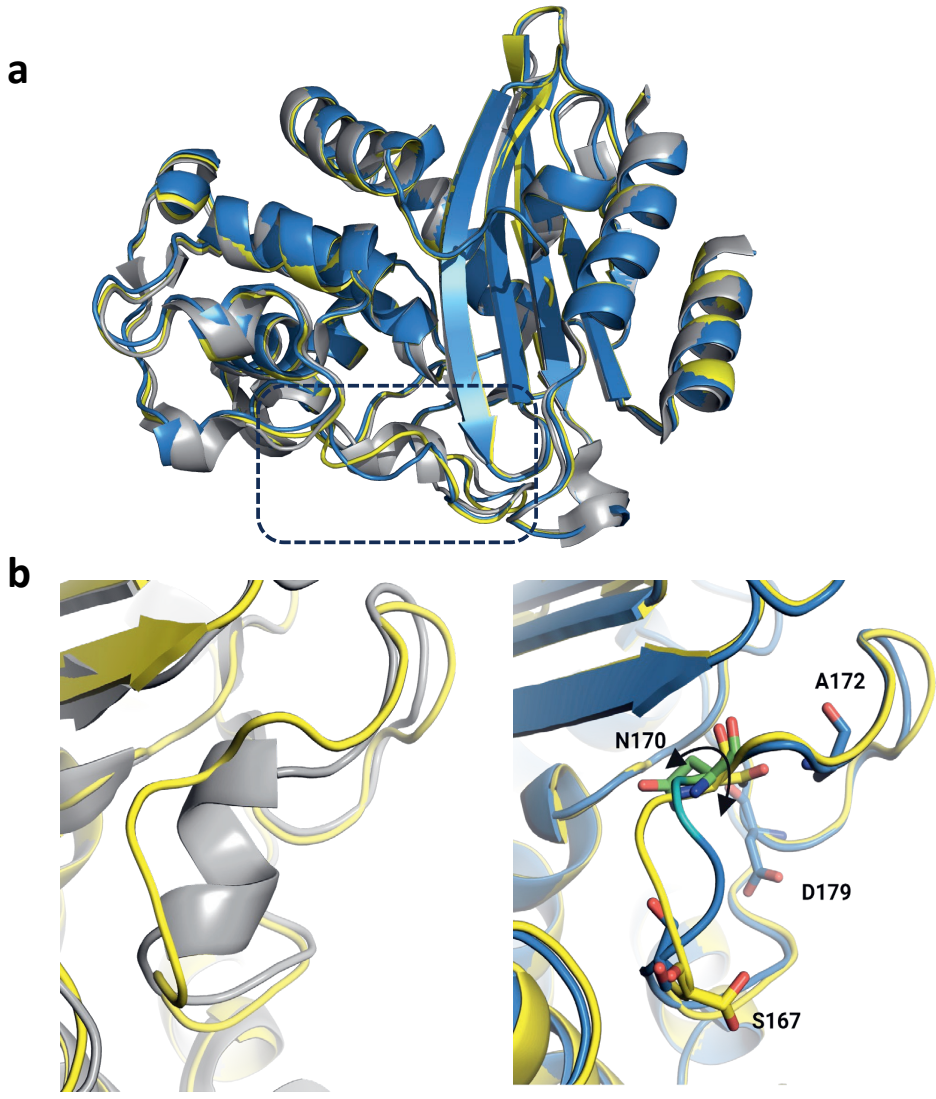

Figure 4.5 Crystal structures of BlaC P167S/D240G (PD) and P167S/D240G/D172A/S104G (PDDS). **a)** X-ray crystal structure of PD (yellow) and PDDS (blue) overlaid with the wild-type structure (grey, PDB 2GDN[72]); **b)** Close-up view of the Ω-loop. The overlap of PD (yellow) and WT (grey) is shown in the left panel. The right panel shows the overlay of PD (yellow) and PDDS (blue). Key residues in the Ω-loop are labelled and shown in sticks. Asn170 is shown in green and the black arrow indicates a flipped peptide bond.

Discussion

The directed evolution experiments demonstrate that a large improvement of the ceftazidime activity is achieved in a few rounds of mutation and selection, evidence for the evolutionary adaptability of BlaC toward new antibiotics. Evolution at 23 °C and 37 °C yields different variants, which is to be expected given the randomness of the mutagenesis process. The introduction of a first mutation changes the epistatic background meaning that different evolutionary paths may be followed from then onward. Mutants originating from low-temperature evolution show better resistance at low temperatures than those derived from high-temperature evolution. These results suggest that the variants evolved at low temperatures are more optimized for this condition. However, all variants show more ceftazidime activity, both in cells and as purified proteins, at 37 °C than at 23 °C, even if they were evolved at 23 °C. This appears counter-intuitive because it was expected that high temperature, not low temperature is the stronger selection force. However, the fact that these experiments were done in *E. coli*, which is a mesophilic bacterium thriving in the optimal temperature range of 35 ℃ to 40 ℃, may have affected the results; growing at lower temperature causes more stress, resulting in overall lower antibiotic resistance and therefore stronger selection pressures. It is speculated that the reason that all mutants are active at 37 °C is that the thermostability of BlaC is too high to influence evolution at 37 °C. Melting temperatures were measured between 50 °C and 62 °C (for WT BlaC). Unfolding is highly cooperative and therefore occurs over a small temperature range. As a consequence, a temperature of 37 °C may still not impose significant selection pressure during the evolutionary process.

Interestingly, however, the melting temperatures of the variants, increase in the last rounds of evolution, after having gone down initially. Given that stability did not appear to be an issue during the evolution at either temperature, it is concluded that this increase in the melting temperature could be a side-effect of the optimization of enzyme activity, which is somewhat counter intuitive because usually, evolution of enhanced activity usually leads to reduced stability.[5,157,212,213] The NMR results may explain this observation. The successive variants display a shift toward a single conformational state. The introduction of P167S changes the structure of the Ω-loop,

resulting in the appearance of a second state for the resting state of the enzyme, further evolution stabilizes this state at the cost of the original state that is similar to WT BlaC at neutral pH. The crystal structure of evolved mutants also displays the flexibility of the Ω-loop, indicating that stabilizing the structure of the Ω-loop would reduce the dynamics of the enzyme. Thus, the directed evolution enhances the population of the state that is most active against ceftazidime. This reduction in the entropy of the enzyme may also explain the increased thermostability because the enzyme has become less dynamic. Furthermore, it explains the observed trade-off in nitrocefin activity because the new state has reduced activity toward this substrate due to displacement of Glu166, required for hydrolysis of nitrocefin but not ceftazidime (see Chapter 3).

Materials and Methods

Construction of random mutant library

The library for the template was constructed by carrying out by error-prone polymerase chain reactions (EP-PCR), which were performed using an *E. coli* expression-optimized *blaC* gene [179] encoding a TAT signal sequence for translocation to the periplasm. The signal sequence was not mutated. DreamTaq DNA.[214] The following temperature-controlled program was used for EP-PCR: an initial denaturation step (95 °C for 3 min), fifteen amplification cycles (denaturation at 95 °C for 30 s, annealing at 60 °C for 30 s, and extension at 72 °C for 3 min) and a final extension step (72 °C for 5 min). For the directed evolution, plasmids from clones selected from a preceding evolutionary round were subjected by EP-PCR with GeneMorph II Random Mutagenesis Kit. To balance the mutation frequency, the initial amount of *blaC* gene was varied from 100 ng and 800 ng (100 ng, 200 ng, 400 ng, and 800 ng). After checking on the gel and normalizing the concentration of the libraries, they were mixed to keep the diversity of the libraries. The reaction was done with initial denaturation at 95 °C for 2 min and followed by 30 cycles of denaturation at 95 °C for 30 s, annealing at 60 °C for 30 s, and extension at 72 °C for 3 min.

In vivo selection

The mutated blaC genes libraries were cloned behind the lac promotor in pUK21 through restriction and ligation using *Bgl*II and *Xho*I restriction sites. *E. coli* KA797 cells were transformed with the plasmid library and plated on lysogeny broth (LB) agar plates with kanamycin (50 μg/mL), isopropyl β-D-1-thiogalactopyranoside (IPTG, 1 mM), and various concentrations of ceftazidime to screen (1 μg/mL, 10 μg/mL, 25 μg/mL, 40 μg/mL, and 60 μg/mL). The plates for the template were incubated at 23 °C, 30 °C or 37 °C, for 3 days, 18 hours and 12 hours respectively. Around 5×10^5 clones were screened at each temperature, and three blaC clones were found on the plate incubated at 30 °C. For following directed evolution selection, the plates for template were incubated at 23 °C or 37 °C. Around 1×10^7 clones were screened at each temperature per round selection. Colonies were transferred to LB liquid cultures and incubated overnight at 37 °C and 250 rpm. Plasmids were isolated

and transformed into fresh KA797 cells to confirm that resistance was the result of mutations in the blaC gene and not due to changes of the host cell. The mutated *blaC* genes were verified by DNA sequencing.

Antimicrobial susceptibility testing

Antibiotic resistance was tested in the *E. coli* cells carrying pUK21-*blaC* plasmids with the gene behind the *lac* promotor. Drops of 10 µL of *E. coli* cultures with optical densities (OD_{600}) of 0.3, 0.03, 0.003 and 0.0003 were applied on the LB plates containing 50 µg mL^{-1} kanamycin and 1 mM IPTG, and various concentrations of ceftazidime (15 µg mL^{-1} to 60 µg mL^{-1}). The plates were incubated at 23 °C or 37 °C until growth was visible and imaged by Gel Doc XR+ (Bio-Rad) and ImageLab version 6.0.1 (Bio-Rad).

BlaC production

The genes for all BlaC mutants were cloned into pET28a+ plasmids downstream of an N-terminal His-tag with T7 promotor and a TEV cleavage sit by site-mutagenesis (Gibson assembly method). The presence of the mutations was confirmed by sequencing. *E. coli* strain Bl21pLysS (DE3)[179] and pET28a+ based plasmids were used for overproduction of the mutant protein in the cytoplasm.[179] Cells were cultured in LB medium at 37 °C with 50 µg mL^{-1} kanamycin and 34 µg mL^{-1} chloramphenicol until the OD_{600} to 0.6-0.8 and were induced with 1 mM IPTG, followed by incubation of the cultures at 18 °C overnight. The proteins were purified according to previously described protocols.[149] Pure protein was stored at -80 °C in 100 mM sodium phosphate (pH 6.5). For determination of the amount of soluble protein, the OD_{600} of the overnight culture was adjusted to 1 and 500 µL was centrifugated and resuspended in 50 µL B-PER (Thermo Scientific) for lysis. After 30 minutes of incubation at room temperature, 30 µL was treated with SDS-PAGE cracking buffer (20 mM Tris/HCl pH 6.8, 5 mM EDTA, 0.5% SDS, 0.1% β-mercaptoethanol). The soluble and lysate fraction samples were analyzed by running on a 4-15% Mini-PROTEIN TGX Stain Free Protein SDS-PAGE gels. The signal intensity of the band corresponding to BlaC for each mutant was compared to the signal intensity of WT BlaC using ImageLab software (BioRad). The experiment was done in triplicate to calculate the expression

level.

Thermal stability

The thermal stability of BlaC mutants was determined by tryptophan fluorescence changes as a function of temperature using a Tycho NT.6 (NanoTemper Technologies, München, Germany) at 330 nm and 350 nm. The ratio 330 nm/350 nm was used to evaluate the melting temperature. All measurements were done in triplicate in 100 mM sodium phosphate buffer at pH 6.5.

Enzyme kinetics

In vitro kinetic parameters were determined by monitoring the absorption change at 486 nm for nitrocefin ($\Delta\varepsilon_{486}$ = 18000 $M^{-1}cm^{-1}$)[188] with a TECAN infinite® M1000PRO plate reader at 25 °C, 30 °C, and 35°C. All measurements were performed in triplicate, 200 nM BlaC mutants were used, and the reaction was followed for 5 min. The initial velocities were fitted to the Michaelis-Menten equation 4.1:

$$v_{\mathrm{i}} = \frac{k_{\mathrm{cat}}[E][S]}{K_{\mathrm{M}}+[S]} \tag{4.1}$$

Where v_i is the initial velocity, k_{cat} is the turnover number and K_M is the apparent Michaelis constant. The hydrolysis reaction comprises several steps, so the definition of this constant differs from the standard one and is thus considered an apparent K_M. The extinction coefficient for ceftazidime ($\Delta\varepsilon_{260}$ = 7 ± 1 $mM^{-1}cm^{-1}$) was determined using a thermostatic PerkinElmer Lambda 1050+ UV-Vis spectrometer. To study ceftazidime hydrolysis, 80 nM of BlaC variants was incubated with 25 µM ceftazidime and absorbance change at λ_{260} was measured for 5 min. Due to the high $K_{\mathrm{M}}^{\mathrm{app}}$ values, the V_{max} cannot be determined. To obtain an estimate for k_{cat}/K_M, eq. 4.2 was used[100], as the limiting case of eq. 4.1 ([S] << K_M), to determine the catalytic efficiency ($k_{\mathrm{cat}}/K_{\mathrm{M}}$):

$$v_{\mathrm{i}} = \frac{k_{\mathrm{cat}}}{K_{\mathrm{M}}}[E][S] \tag{4.2}$$

Where v_i represents initial velocity and [E] and [S] are the concentrations of enzyme and substrate used, respectively. All kinetic measurements were performed in triplicate in 100 mM NaPi buffer at 10 °C, 15°C, 20°C, 25°C, 30°C, and 35 °C.

NMR spectroscopy

Backbone assignments for [^{15}N, ^{13}C] BlaC mutants were obtained with standard HNCA and TROSY-HSQC experiments that were recorded on a Bruker AVIII HD 850 MHz spectrometer with a TCI cryoprobe at 25 °C in 100 mM sodium phosphate buffer (pH 6.5), with 1 mM TSP (trimethylsilylpropanoic acid) and 6% D_2O in Shigemi tube. Data were processed with Topspin 4.1.1 (Bruker Biospin) and analyzed using CcpNmr version 2.[161] The spectrum was assigned with the HNCA and the WT spectra at pH 6.5 (BMRB ID: 27067),[149] and confirmed with the HNCA spectrum. The average chemical shift differences $\Delta\delta$ between the two states observed for BlaC of the ^{1}H ($\Delta\delta_1$) and ^{15}N ($\Delta\delta_2$) resonances of backbone amides were calculated with equation 4.3.

$$\Delta\delta = \sqrt{\frac{1}{2}\left[{\Delta\delta_1}^2 + \left(\frac{\Delta\delta_2}{5}\right)^2\right]} \tag{4.3}$$

For the temperature titration, samples were prepared in 100 mM sodium phosphate at pH 6.5 (with the addition of 6% D_2O and 1 mM trimethylsilylpropanoic acid). A series of 2D [^{1}H, ^{15}N] HSQC spectra were recorded at five temperatures ranging from 283 to 303 K (283 K, 288 K, 293 K, 298 K, and 303 K) to determine the population of states and temperature sensitive region.

Protein crystallization

Crystallization conditions for BlaC mutant P167S/D240G and P167S/D240G/ /D172A/S104G (PDDS) at a concentration of 12 mg mL^{-1} were screened by the sitting-drop method using the JCSG$^+$, BSC, PACT, and Morpheus (Molecular Dimensions, Catcliffe, UK) screens at 20 °C with 200 nL drops with a 1:1 protein to screening condition ratio. Crystal of BlaC P167S/D240G (PD) was grew in 0.1 M sodium cacodylate at pH 6.07 with 1.16 M trisodium citrate as precipitant. A crystal

of BlaC P167S/D240G/S104G/D172A grew within two weeks in 0.1 M Bis-Tris buffer, pH 5.5 and 2 M $(NH_4)_2SO_4$ as additive. After one month the crystals were mounted on cryoloops in mother liquor, with the addition of 30% glycerol and flash frozen in liquid nitrogen for X-ray data collection.

Data collection, processing, and structure refinement

Diffraction data for the BlaC mutant P167S/D240G and P167S/D240G/D172A/S104 G (PDDS) mutant structures were collected at the European Synchrotron Radiation Facility on the MASSIF beamline.[209] The resolution cutoff was determined based on completeness and CC1/2 values. The data were indexed and integrated using DIALS[209] and scaled using Aimless.[168] The structures were solved by molecular replacement using MOLREP from the CCP4 suite by the PDB entry 2GDN[72] as the model for molecular replacement. Model building and refinement were performed in Coot and REFMAC. Waters were added in REFMAC during refinement. The models were further optimized using the PDB-REDO web server. The refinement and data collection statistics are given in the supplementary information (Table S4.3). The structures P167S/D240G and P167S/D240G/S104G/D172A have been deposited in the Protein Data Bank.

Supporting information

Figure S4.1 Activity against ceftazidime of evolved BlaC mutants at 37 ℃, wild-type BlaC, and inactive S70A BlaC as the negative control. Cultures of *E. coli* expressing genes of the BlaC variants were spotted in the increasing dilution on the plates containing various concentration of ceftazidime. All the plates contain kanamycin (50 μg mL^{-1}) to ensure plasmids stability and 1 mM IPTG to induce gene expression.

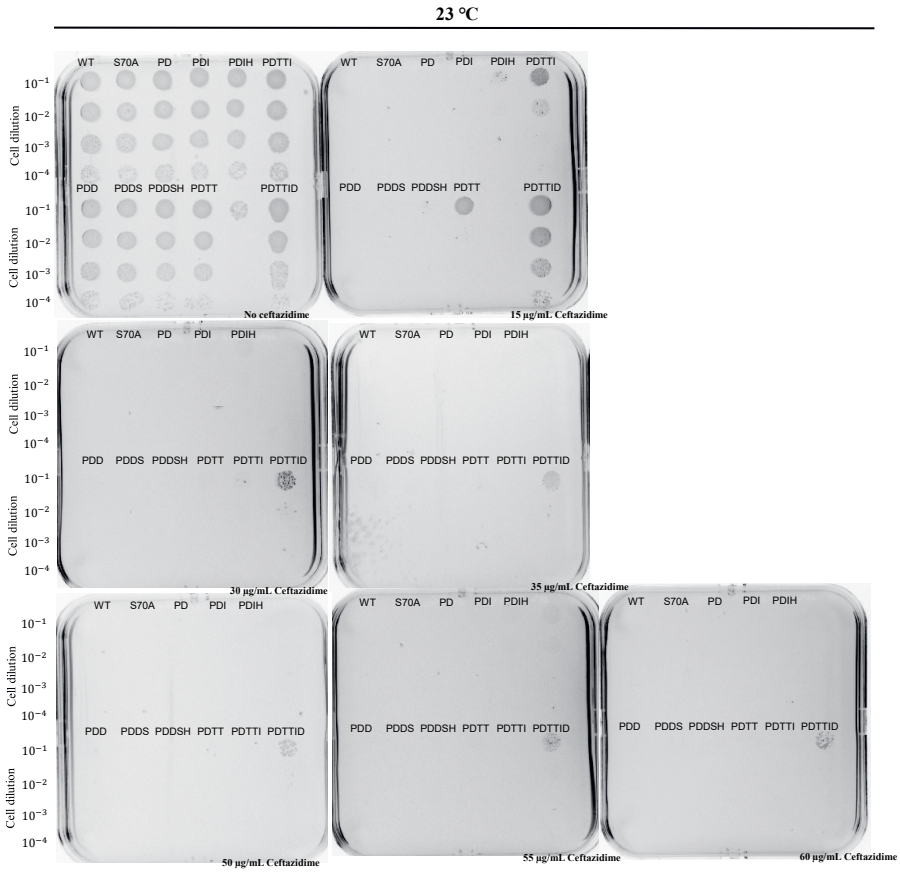

Figure S4.2 Activity against ceftazidime of evolved BlaC mutants at 23 °C, wild-type BlaC, and inactive S70A BlaC as the negative control. Cultures of *E. coli* expressing genes of the BlaC variants were spotted in the increasing dilution on the plates containing various concentration of ceftazidime. All the plates contain kanamycin (50 µg mL^{-1}) to ensure plasmids stability and 1 mM IPTG to induce gene expression.

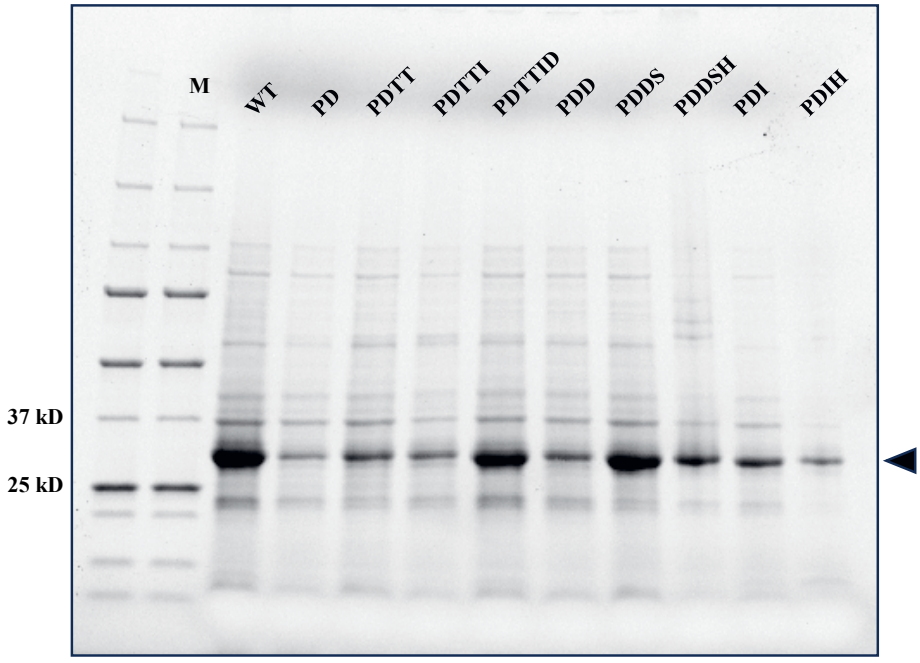

Figure S4.3 SDS-PAGE gel analysis shows the soluble fractions of cell cultures producing WT and mutant BlaC. The arrow indicates the position of BlaC at 31 kDa.

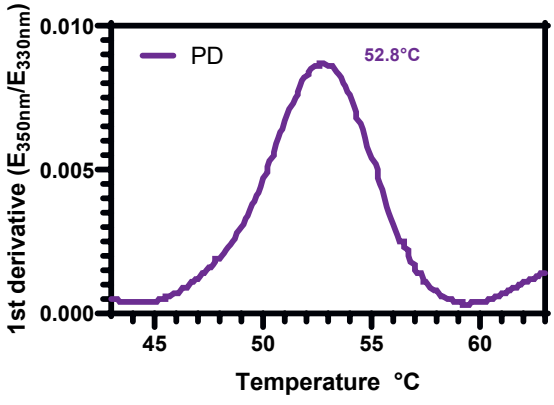

Figure S4.4 The derivative signal from Trp fluorescence as a function of temperature for the BlaC P167S/D240G mutant. The melting temperature is also listed in Table 4.1.

Table S4.1 MIC of ceftazidime conferred by BlaC wild-type and mutants. G, Generation; Temp, temperature at which variant was evolved.

Mutations	G	Temp (℃)	MIC (μg/mL) for ceftazidime		
			23℃	30℃	37℃
WT			0.3	<0.5	0.5
P167S/D240G	0	30	4	8	4
P167S/D240G/I105F	1	37	8	30	16
P167S/D240G/I105F/H184R	3	37	15		>60
P167S/D240G/T208I/T216A	1	23	20		<60
P167S/D240G/T208I/T216A/I105F	2	23	35		60
P167S/D240G/T208I/T216A/I105F/D176G	3	23	>60		>60
P167S/D240G/D172A	1	37	<15		35
P167S/D240G/D172A/S104G	2	37	<15		45
P167S/D240G/D172A/S104G/H184R	3	37	15		>60

Table S4.2 Kinetic parameters for ceftazidime hydrolysis by wild-type and mutant BlaC at temperature increased. The errors are the standard deviation over duplicate experiments.

BlaC variants	10℃	15℃	20℃	25℃	30℃	35℃
	k_{cat}/K_M^{app} (10^3 $M^{-1}s^{-1}$)					
Wildtype (WT)	0.23 ± 0.07					
P167S/D240G	0.4 ± 0.2	2.5 ± 0.6	2.8 ± 0.8	12.0 ± 3.4	6.7 ± 0.8	6.4 ± 1.1
P167S/D240G/T208I/T216A	26.7 ± 5.6	20.2 ± 3.5	29.8 ± 4.7	31.9 ± 4.1	43.6 ± 5.2	52.3 ± 6.2
P167S/D240G/T208I/T216A/I105F/D176G	56.2 ± 6.9	65.0 ± 6.3	77.4 ± 8.9	90.1 ± 5.3	106 ± 8.7	110 ± 10.1
P167S/D240G/D172A	12.5 ± 3.0	15.9 ± 4.8	17.5 ± 3.9	25.1 ± 2.3	28.6 ± 4.2	29.1 ± 2.8
P167S/D240G/D172A/S104G/H184R	27.4 ± 4.2	43.9 ± 4.7	47.2 ± 4.0	40.5 ± 6.4	46.5 ± 4.8	56.2 ± 6.2
P167S/D240G/I105F	21 ± 3					

Table S4.3 Data collection and refinement statistics for the structures of BlaC mutants

Data collection	P167S/D240G	P167S/D240G/T208I/T216A
Wavelength (Å)	0.98Å	0.87Å
Resolution (Å)	54.45 (1.32) 1.30-1.32	38.44 (1.6) 1.60-1.63
Space group	P1 21 1	P1 21 1
Unit cell a, b, c (Å)	38.90 54.45 53.94	38.88 54.64 54.16
Unit angle α, ß, γ	90.0 92.4 90.0	90.0 93.1 90.0
CC1/2	99.5 (45.5)	99.8 (86.1)
Rpim (%)	6 (55.1)	3.4 (29.2)
|I/σI|	7.2 (2.1)	14.7 (1.5)
Completeness (%)	99.5 (97.7)	67.5 (7.8)
Multiplicity	3.1	1.8
Unique reflections	55106	20143
Refinement		
Atoms protein/ligands/water	2050/13/250	1978/0/169
B-factors protein/ligands/water ($Å^2$)	12/9/15	20/0/28
R_{work}/R_{free} (%)	13.5/16.0	17.2/20.6
Bond lengths RMSZ/RMSD (Å)	0.794/0.013	0.297/0.01
Bond angles RMSZ/RMSD (Å)	0.84/1.81	0.54/1.46
Ramachandran plot preferred/outliers	252/3	248/3
Ramachandran plot Z-score	0.049	0.142
Clash score	7.48	3.3
MolProbity score	1.47	1.38